Robust Multi-spectral Imaging For Ocular Biometric

Narayan Vetrekar,[a,b*] R. Raghavendra,[b*], Kiran B. Raja,[b*] R. S. Gad,[a] Christoph Busch[b]
[a]Department of Electronics, Goa University, India
[b]Norwegian Biometrics Laboratory, NTNU - Gjøvik, Norway
[a]{elect.ntvetrekar; rsgad} @unigoa.ac.in
[b]{narayan.t.vetrekar; raghavendra.ramachandra; kiran.raja; christoph.busch} @ntnu.no

Abstract

Recent development of sensors has allowed the biometric community to explore the possibility of authentication beyond visible spectrum. More importantly, multi-spectral imaging in biometric has shown great potential to work robustly under unknown varying illumination conditions for face recognition. While face biometrics in traditional settings has also indicated the applicability of ocular region for improving the performance, there are not many works that have explored recent imaging methodologies. In this paper, we present the study that explores the possibility of recognizing ocular biometric feature using multi-spectral imaging. While exploring the possibility of recognizing the periocular region in different spectral bands, this work also presents the performance variation of periocular region for cross-spectral matching. We have captured a new ocular image database in $eight$ narrow spectral bands across Visible (VIS) and Near-Infra-Red (NIR) spectrum ($530nm$ to $1000nm$) using our custom built sensor. The data consists of images from 52 subject with a sample size of 4160 spectral band images captured in two different sessions. The extensive set of experimental evaluation results obtained on the state-of-the-art methods indicates highest recognition rate of 96.92% at $Rank-1$, demonstrating the potential of multi-spectral imaging for robust periocular recognition.

1. Introduction

Among the physiological biometric traits, ocular biometric has been significantly explored in the last few years, due to it's reasonable recognition accuracy and stable biometric features [2]. Essentially, the significant progress of iris recognition has made ocular biometric a popular trait among the biometric community, which has resulted in number of methodologies developed to explore the discriminative information present across the ocular region for robust performance [11]. Further, related research have witnessed number of contributions using various ocular regions especially iris [5], retina [6] , sclera [13] and periocular region [11] as potential biometric traits in chronological order of their existence [8]. The success of ocular biometrics has resulted further in installation of number of ocular biometric systems which either uses one of the above mentioned ocular regions for verification or identification of individuals [8].

Periocular region is defined as a small region surrounding the eye that contains the essential fine texture and geometric information compared to other facial parts. Periocular has received a significant attention in the scenario where other ocular regions cannot be captured in the non-idealistic conditions. For instance, collecting iris sample is challenging when subjects blinks eye or under non ideal pose angle, which commonly results in noisy sample data [3]. Unlike iris, which depends on NIR imaging sensor, periocular region is basically segmented from the face images, with most of the face biometric systems relies on face images captured in visible spectrum, majority of work carried out in the direction of periocular recognition are based on visible spectrum data [10]. Further, the recent work also indicates the use of Visible(VIS), Near Infra Red(NIR), Short Wave Infra Red(SWIR), Mid Wave Infra Red (MWIR) and Long Wave Infra Red (LWIR) spectrum for periocular matching and cross spectral periocular comparison[12].

Most of the earlier works were carried out extensively on visible spectrum data, with limited attempts using Near-Infra-Red (NIR) spectrum, Short Wave Infra Red(SWIR), Mid Wave Infra Red (MWIR) and Long Wave Infra Red (LWIR) spectrum for periocular matching. To best of our knowledge, the potential of multi-spectral imaging [1] has not been explored extensively for periocular biometrics. Multi-spectral imaging captures the set of spectral band images across wide electromagnetic spectrum such that the discriminative characteristic band information can be obtained for robust performance. The idea of using

*The authors have contributed equally in this paper.

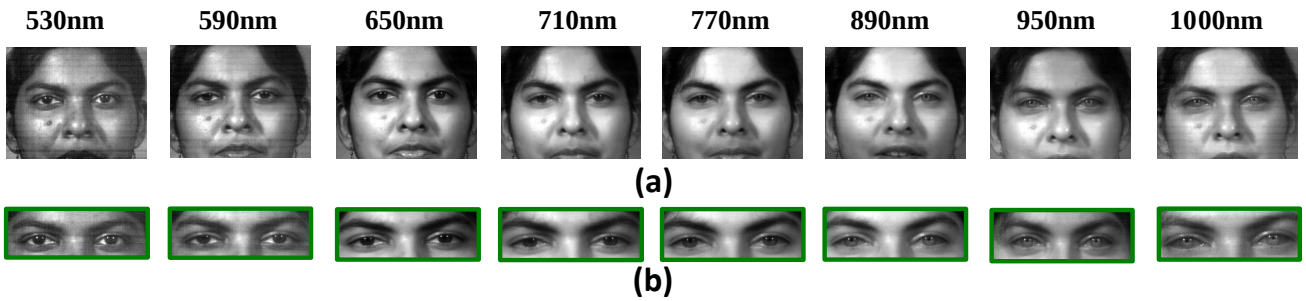

Figure 1: Multi-spectral images captured for periocular biometric: (a) Original spectral images acquired from multi-spectral sensor, (b) Segmented periocular region for individual spectral band

multi-spectral imaging approach is to explore the complementary image information in the form of reflectance and emittance data by characterizing the spectral properties of multi-spectral imaging sensor. The reasonable accuracy and the success of multi-spectral imaging to extract the useful $spatio$-spectral data have resulted into its use case in different biometric trait recognition [14].

In this paper, we have introduced multi-spectral imaging for robust periocular biometric authentication. More specifically, we have acquired multi-spectral data for periocular biometrics from 52 subjects collected in $eight$ narrow spectral bands spanning from Visible (VIS) to Near-Infra-Red (NIR) wavelength range (Details are given in Section 2). The data acquired in two different session corresponds to the total of 4160 sample spectral band images. To explore the significance of multi-spectral imaging, we present an extensive set of experimental results across individual spectral bands for periocular matching using state-of-the-art methods. Further, cross spectral comparison results are also presented in this work to analyze the performance of periocular matching under different spectrum. The experimental results are presented in terms of recognition rate at $Rank-1$ and graphically using Cumulative Match Characteristic (CMC). The major contribution of this paper are as follows:

1. Presents a study exploring multi-spectral imaging for robust periocular biometric recognition based on the state-of-the-art feature extraction and classifier methods.

2. Introduces a newly captured multi-spectral image database for periocular recognition, which consists of a total of 4160 sample spectral band images from 52 subjects captured in two different sessions. The acquired data consists of $eight$ spectral bands which includes $530nm$, $590nm$, $650nm$, $710nm$, $770nm$, $890nm$, $950nm$ and $1000nm$ band.

3. Presents an extensive set of experimental results in terms of recognition rate at $Rank-1$ for multi-spectral periocular recognition across individual bands independently as well as for cross spectral band matching.

Rest of the paper is organized as follows: Section 2 present in detail, the description of multi-spectral image database collected for periocular biometric. Section 3 explains in brief the state-of-the-art feature extraction and classifiers used in the evaluation of this work. Section 4 details the experimental evaluation protocol and experimental results on the collected multispectral database to explore periocular matching. Section 5 presents the conclusions from this work.

2. Multi-spectral Periocular Database

In this section of the paper, we present the detailed description of multi-spectral periocular database employed in this work. The database is collected using in-house and custom built multi-spectral imaging sensor, which can capture $eight$ narrow spectral band images in Visible (VIS) and Near-Infra-Red (NIR) spectrum. The $eight$ spectral band images captured using the multi-spectral imaging sensor consists of $530nm, 590nm, 650nm, 710nm, 770nm, 890nm$, $950nm$ and $1000nm$ bands. In total, the database consists of images from 52 subjects, collected in two different sessions. A reasonable time difference of 3 to 4 weeks have been maintained between the two sessions. For each subject, we have collected 5 sample images in $eight$ spectral band, which corresponds to 52 $subjects \times 2$ $sessions \times 5$ $samples \times$ 8 $bands$ to obtain the total of 4160 sample images. Further, each sample is acquired at a distance of roughly $1-mts$ from the face of subject in controlled illumination conditions.

2.1. Periocular segmentation and Normalization

The multi-spectral image database acquired for periocular recognition is segmented using both the eye coordinates. In order to obtain the coordinates of left and right eye, we employed face landmark detection technique [17] in this

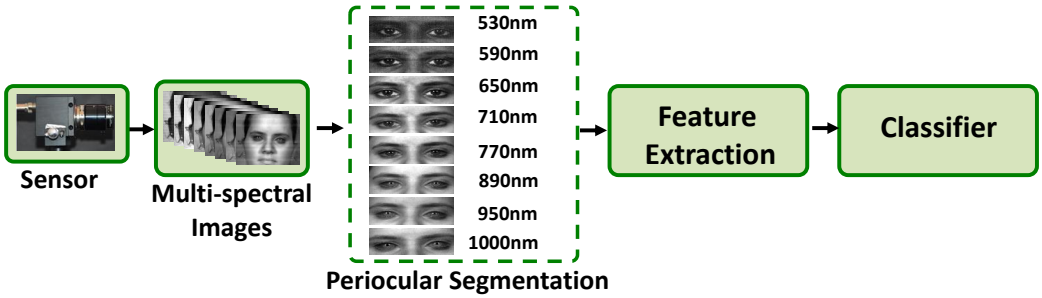

Figure 2: Feature extraction and classification framework

work. Using the eye coordinates, we first performed image normalization, which basically consists of image rotation and translation correction before segmenting the periocular region. The normalized image is cropped for periocular region, which is then resized to a common spatial resolution of 120×240 dimension. Further, an histogram equalization is performed to enhancement the features of periocular images before using it for experimental evaluation.

3. Feature Extraction and Classifier

In this section of paper, we discuss in brief the feature extraction techniques and a feature classifier employed for the experimental evaluation. Specifically, we have employed the state-of-the-art feature extraction methods such as Histogram of Orientated Gradient (HOG)[4], GIST[9], Log-Gabor transform [15] and Binarized Statistical Image Features (BSIF)[7]. These feature extraction methods have been widely used to extract the local and global features in periocular biometrics. Further, to classify the features, we have employed Collaborative Representation Classifier (CRC) [16] to efficiently classify the discriminative features in robust manner. A brief description of each of these methods are given in the following subsections.

3.1. Histogram of Oriented Gradient (HOG)

Histogram of Oriented Gradient (HOG)[4] is a local feature descriptor technique, which depends on the magnitude of gradient vectors. In principle, HOG computes the magnitude of gradient vector by exploring the direction in which the most dominant edges are present. The final histogram feature vector is obtained by placing the magnitude data of each edge in $nine$ bins with each bin size corresponds to 20 degrees spanned from 0 to 180 degrees. Thus, for image size of 120×240 we obtained histogram feature vector of size 1×14616, which corresponds to $405 blocks \times 4 histogram \times 9 bins$.

3.2. GIST

GIST [9] was proposed to explore local and global features for recognizing the object in a given image. The method employs set of Gabor filters having different $scale$ and $orientation$ to extract the useful data of image in the form of feature maps. For this set of experimental evaluation, we employed 4 different $scales$ and 8 different $orientations$ to obtain 32 Gabor fiters, which corresponds to 32 feature maps containing discriminative information across the periocular regions. Further, each feature map is divided into 16 feature maps of 4×4 grids and each 16 feature maps are averaged to obtain final histogram vector of 1×512 dimension that are resulted from $16 averaged\ feature\ maps \times 32 = 512$.

3.3. LogGabor Transform

In the similar line with GIST, LogGabor is another robust feature descriptor that uses banks of Gabor filters of different $scale$ and $orientation$ [15]. Logabor transform combines all the feature matrix obtained across the bank of filters by simply concatenating them to obtain the final feature descriptor. To evaluate this technique, we again employed 32 Gabor filters consisting of 4 different $scales$ and 8 different $orientations$. In this work, for image size of 120×240, we obtained 1×921600 feature dimension corresponds to $(32 FilterBanks) \times (120 \times 240)$, which we further down sample by six times to reduce the computational expenses such that the final feature vector results into 1×153600 dimension.

3.4. Binarized Statistical Image Features (BSIF)

BSIF is another texture descriptor method based on the set of predefined statistical filters learned from natural images[7]. The employed set of filters are convolved with image in holistic manner. Further, by simple binary to gray image conversion operation is employed to combine the binarized statistical filtered image. In this work, we have employed statistical filters of size 17×17 with bit length of 12. The final feature descriptor in the form of histogram

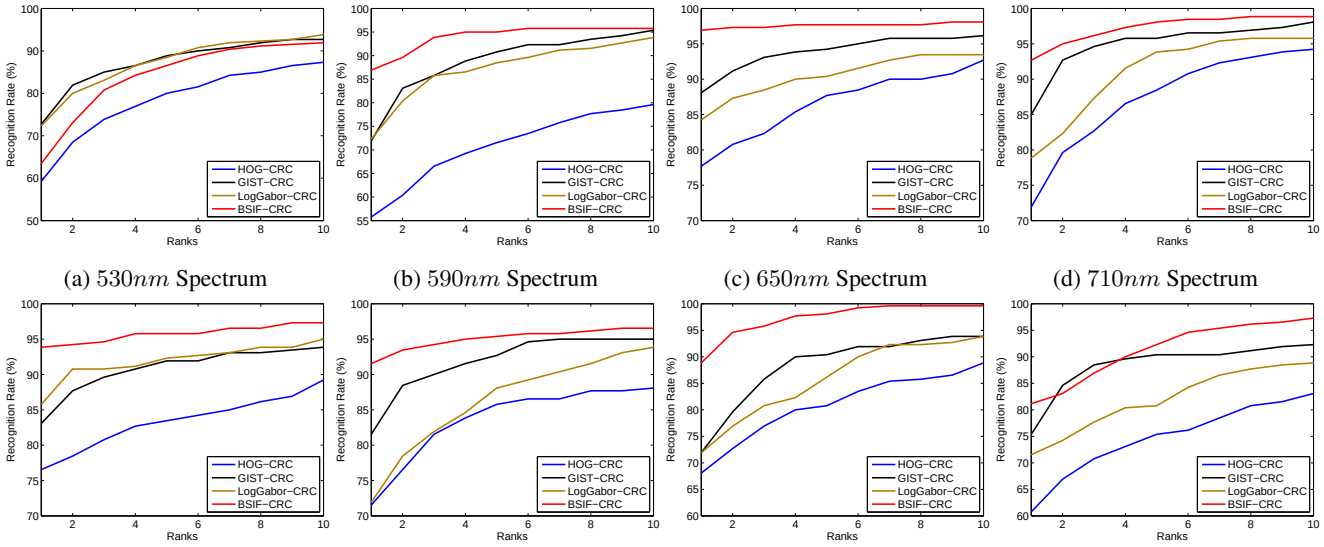

(a) $530nm$ Spectrum (b) $590nm$ Spectrum (c) $650nm$ Spectrum (d) $710nm$ Spectrum

(e) $770nm$ Spectrum (f) $890nm$ Spectrum (g) $950nm$ Spectrum (h) $1000nm$ Spectrum

Figure 3: CMC plot indicating the performance of state-of-the-art methods on individual spectral band (Results are best viewed in color).

features vector of size 1×4096 is obtained for final evaluation of the experiment.

3.5. Collaborative Representation Classifier (CRC)

In order to efficiently classify the histogram feature vectors obtained independently from different feature descriptors mentioned above, we employed a robust Collaborative Representation Classifier (CRC)[16] technique in this work. CRC in principle computes the maximum likelihood ratio of probe sample image with other classes in a joint manner. Further, the final feature classification is performed by simply computing the maximum likelihood of probe sample against the other classes from the gallery set.

Let the set of multi-spectral periocular image is represented as $S_\lambda \in \Re^{m \times n}$, where, λ be the wavelength corresponding to $eight$ different bands $(530nm, 590nm, 650nm, 710nm, 770nm, 890nm, 950nm, 1000nm)$ and $m \times n$ indicates the image dimension. Let the histogram feature vectors computed for S_λ using above different feature descriptor methods be R_λ. To employ CRC, the extracted feature vectors R_λ are learned in a collaborative sub-space ρ_λ and the final comparison scores are obtained using regularised Least Square Regression coefficients on the learned spectral feature vectors against the probe sample image, which is explained mathematically as follows in Equation 1.

$$D = argmin_\beta \left\| P_\lambda - \rho_\lambda \beta \right\|_2^2 + \sigma \left\| \beta \right\|_2^2 \qquad (1)$$

where the P_λ is the feature vector of the probe sample spectral band image, ρ_λ be the learned collaborative subspace corresponds to wavelength λ, β is coefficient vector and σ indicates the regularization parameter. Further, the distance matrix D obtained using Equation 1 is then used as comparison score to obtain the performance matrix.

4. Experiments and Results

This section of paper, we present the experimental evaluation protocol employed on multi-spectral periocular database. The extensive set of experimental results are obtained using state-of-the-art feature extraction algorithms followed by robust Collaborative Representation classifier (CRC). We present the results in terms of recognition rate at $Rank - 1$ and Cumulative Match Characteristic (CMC) plot to demonstrate the significance of multi-spectral imaging for periocular biometrics.

4.1. Experimental protocol

To evaluate the multi-spectral periocular database (Section 2) based on state-of-the-art methods, we present an experimental evaluation protocol that consists of reference set corresponding to sample spectral band images collected from Session 1 and probe set corresponds to sample spectral band images collected from Session 2. Based on this evaluation protocol, we present two sets of experimental results. **Experiment 1** presents the $intra$-band periocular recognition and **Experiment 2** presents the $inter$-band periocular recognition. The detailed analysis of each of these experiments are given in the following sub-sections.

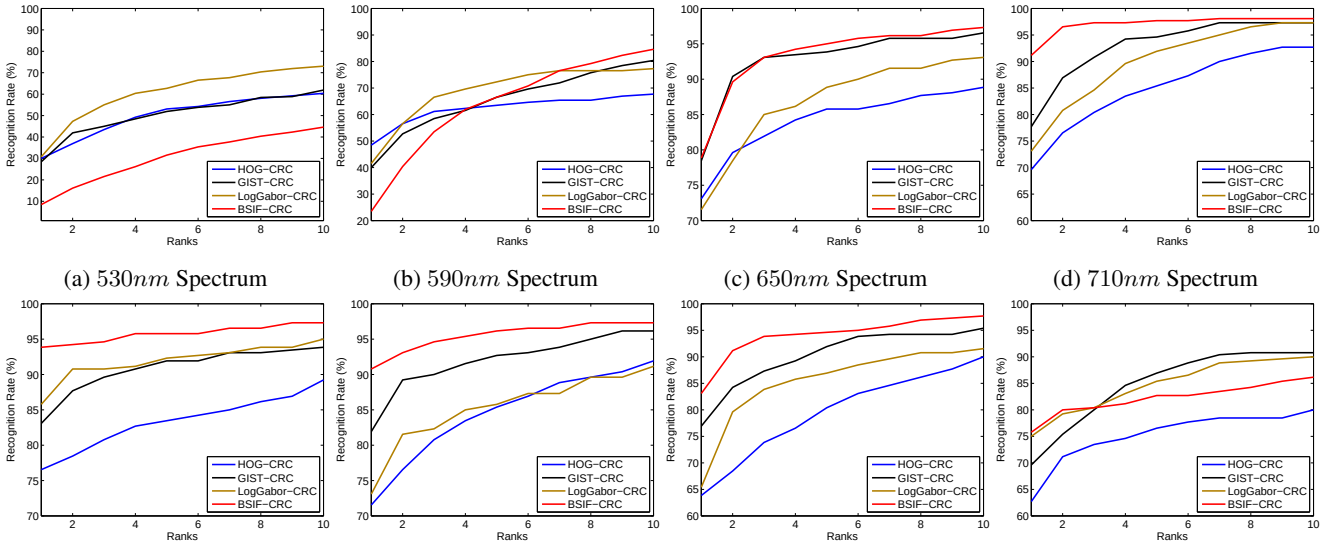

(a) $530nm$ Spectrum (b) $590nm$ Spectrum (c) $650nm$ Spectrum (d) $710nm$ Spectrum

(e) $770nm$ Spectrum (f) $890nm$ Spectrum (g) $950nm$ Spectrum (h) $1000nm$ Spectrum

Figure 4: CMC plots demonstrating the $cross$-spectral performance of algorithms when reference set belongs to (a),(b),(c),(d),(e),(f),(g),(h) and probed against the rest of the bands operated independently. In this plot, results for $770nm$ probe band is shown which is best performing band (Results are best viewed in color).

Table 1: Recognition rate at $Rank-1$ for individual spectral bands.

Algorithm	Bands							
	530nm	590nm	650nm	710nm	770nm	890nm	950nm	1000nm
HOG-CRC	59.23	55.77	77.69	71.92	76.54	71.54	68.08	60.77
GIST-CRC	72.69	71.92	88.08	85.00	83.08	81.54	71.92	75.38
LogGabor-CRC	72.31	72.31	84.23	78.85	85.77	71.92	71.92	71.54
BSIF-CRC	63.46	86.92	96.92	92.69	93.85	91.54	88.85	81.15

4.2. Experiment 1: Intra Band

Experiment 1 presents the $intra$ band performance analysis of multi-spectral periocular database. The purpose of this experiment is to explore the true significance of each of the individual spectral bands for robust periocular recognition. Specifically, the recognition rate is obtained at $Rank-1$ for individual $eight$ spectral bands independently based on the experimental protocol (Section 4.1) . For instance, the individual band (say $530nm$) from Session 1 is considered as reference set and corresponding spectral band (say $530nm$) from Session 2 is used as probe set for the evaluation. Table 1 presents the Rank-1 recognition rate of individual spectral band and Figure 3 illustrates the Cumulative Match Characteristic (CMC) using state-of-the-art methods. Based on the obtained experimental results, we present following major observations:

- The highest $Rank-1$ recognition rate of 96.92% is obtained for $650nm$ spectrum using BSIF-CRC method and the lowest performance of 55.77% recognition rate is obtained for $590nm$ spectrum using HOG-CRC algorithm.
- Of all the state-of-the-art methods employed in this work for multi-spectral periocular recognition, BSIF-CRC outperforms the other algorithms across most of the spectral bands, indicating the potential of statistical filter based techniques for robust performance. Further, HOG-CRC found to be the least performing algorithm across all spectral band compared to other employed methods in this experiment.
- Among the individual spectral bands, $650nm$, $710nm$, $770nm$ presents the outstanding performance using state-of-the-art methods and individual bands $530nm$, $590nm$ performs poorly indicating the need for continued research.

4.3. Experiment 2: Inter Band

The Experiment 2 is based on the $inter$ band performance analysis using multi-spectral periocular images. The goal of this experiment is to demonstrate the performance of $cross$-spectral periocular recognition, in which reference and probe set corresponds to two different spectrum bands. To evaluate this experiment, we keep the reference set fixed (say $530nm$ spectrum) from Session 1 and performance is obtained against the rest of the spectrum bands (say $590nm$, $650nm$, $710nm$, $770nm$, $890nm$, $950nm$, and $1000nm$) from Session 2, when probed independently. Table 2 details

the recognition rate at $Rank-1$ for $inter$-band experimental evaluation and Figure 4 demonstrated the Cumulative Match Characteristics (CMC) for different reference spectrum (The graphical results shown in Figure 4 presents the performance of best performing probe spectrum i.e.$770nm$ band). Based on the experimental results, we deduce our observations as follows:

- BSIF-CRC algorithm demonstrates the outstanding performance for cross spectral comparison, except for the reference set belonging to $530nm$ and $590nm$ spectrum, where most of the other state-of-the-art algorithms also indicate a poor performance.
- The maximum recognition rate of 91.92% at $Rank-1$ is obtained using BSIF-CRC method for $710nm$ and $890nm$ probe spectrum bands, when $770nm$ spectrum band is in the reference set.
- The lowest recognition rate of 8.46% at $Rank-1$ is obtained using BSIF-CRC method for $770nm$ probe spectrum bands, when $530nm$ spectrum band is in the reference set.
- Further, $cross$-spectral comparison indicates the poor $Rank-1$ recognition rate when reference set belongs to $530nm$ and $590nm$ spectral bands.
- The $cross$-spectral comparison indicates reasonable recognition rate at $Rank-1$ when the reference and probe spectrum are close to each other. For instance, when $770nm$ spectrum is in the reference set, the closest probe spectrum i.e. $710nm$ and $890nm$ obtained higher recognition rate of 91.92% for BSIF-CRC algorithm. However for the same reference set, $530nm$ probe spectrum resulted in 29.62% recognition rate. This indicates the fact that the increased difference between reference spectrum and probe spectrum results in drop of the performance of algorithms.

In brief, multi-spectral imaging obtains reasonable recognition accuracy at $Rank-1$ for periocular biometric using state-of-the-art methods. Further, $inter$-band ocular matching is still challenging problem and needs research attention.

5. Conclusion

Ocular biometric has emerged as popular physiological trait due to its reasonable recognition accuracy compared to other biometric traits. The limitations of other ocular regions (such as iris, retina and sclera) to capture the data under uncontrolled environmental conditions has led to the emergence of periocular biometric as alternative trait for robust performance. Further, the recent trend to use multi-spectral imaging for biometric authentication is on the rise by leveraging the discriminative spectral information across various band of electromagnetic spectrum. We introduce in this paper, a multi-spectral imaging approach to explore possibility of periocular matching. A multi-spectral periocular database of 52 Subject is collected in $eight$ narrow spectral bands corresponding to $530nm$, $590nm$, $650nm$, $710nm$, $770nm$, $890nm$, $950nm$, $1000nm$ bands which amounts to 4160 sample images in total. To demonstrate the multi-spectral periocular matching, we have presented two sets of experiments based on state-of-the-art feature extraction and classifier method. The two sets of experiments evaluated in this work correspond to $intra$-band and $inter$-band performance to present the true significance of multi-spectral imaging for robust periocular recognition. The results demonstrate the possible use of multi-spectral imaging for periocular biometrics, with highest $Rank-1$ recognition rate of 96.92% obtained using state-of-the-art method.

Table 2: Recognition rate at $Rank-1$ for $cross$-spectral experiment.

Reference Bands	Algorithm	Probe Bands							
		530nm	590nm	650nm	710nm	770nm	890nm	950nm	1000nm
530nm	HOG-CRC	–	55.00	36.54	22.31	30.00	24.62	23.85	27.69
	GIST-CRC	–	57.31	30.00	28.46	28.46	23.85	20.77	27.31
	LogGabor-CRC	–	63.08	56.54	37.69	30.77	26.54	21.92	30.00
	BSIF-CRC	–	42.31	29.62	12.31	8.46	8.85	11.15	10.77
590nm	HOG-CRC	49.62	–	53.46	50.77	48.46	40.77	38.46	43.08
	GIST-CRC	57.31	–	57.31	49.62	40.00	32.69	30.00	35.77
	LogGabor-CRC	67.69	–	68.46	64.62	41.54	40.38	35.38	40.38
	BSIF-CRC	56.92	–	71.54	47.31	23.46	25.00	24.62	34.23
650nm	HOG-CRC	31.15	64.23	–	83.08	73.08	68.85	63.08	60.00
	GIST-CRC	19.62	56.54	–	84.23	78.46	68.46	61.54	55.77
	LogGabor-CRC	65.77	77.69	–	80.00	71.54	62.69	59.62	63.46
	BSIF-CRC	46.54	82.69	–	91.15	78.85	68.46	67.31	61.54
710nm	HOG-CRC	18.08	48.85	76.15	–	69.62	60.00	55.77	44.23
	GIST-CRC	12.69	46.54	85.00	–	77.69	64.62	57.69	50.00
	LogGabor-CRC	58.46	71.54	81.92	–	73.08	57.69	60.77	50.38
	BSIF-CRC	31.54	70.77	90.38	–	91.15	80.77	72.31	62.69
770nm	HOG-CRC	21.92	58.46	70.00	69.23	–	69.62	66.54	63.85
	GIST-CRC	16.15	41.15	79.62	81.92	–	70.00	69.62	66.92
	LogGabor-CRC	53.46	72.69	77.69	77.69	–	74.23	63.08	75.77
	BSIF-CRC	29.62	54.62	85.00	91.92	–	91.92	70.77	78.08
890nm	HOG-CRC	24.62	51.54	63.46	66.15	71.54	–	60.38	58.85
	GIST-CRC	15.00	37.69	69.23	77.69	81.92	–	66.15	70.00
	LogGabor-CRC	43.08	52.69	64.23	70.77	73.08	–	54.23	67.69
	BSIF-CRC	30.00	49.62	73.46	79.62	90.77	–	72.69	84.23
950nm	HOG-CRC	12.69	51.15	61.54	63.85	63.85	62.31	–	62.31
	GIST-CRC	17.31	40.38	66.92	68.85	76.92	73.46	–	65.38
	LogGabor-CRC	47.31	62.69	70.38	73.46	65.38	63.46	–	68.46
	BSIF-CRC	20.00	44.62	75.77	82.31	83.08	82.31	–	84.62
1000nm	HOG-CRC	18.46	48.85	63.85	58.08	62.69	58.46	62.69	–
	GIST-CRC	20.77	43.85	58.85	59.62	69.62	68.85	71.54	–
	LogGabor-CRC	42.31	53.46	65.77	60.77	75.00	63.85	61.92	–
	BSIF-CRC	19.23	43.46	60.77	59.62	75.77	70.77	71.92	–

6. Acknowledgment

The work is supported by University Grant Commission, India (Grant No.40-664/2012(SR) and Research Council of Norway (Grant No. IKTPLUSS 248030/O70).

References

[1] T. Bourlai and B. Cukic. Multi-spectral face recognition: Identification of people in difficult environments. In *Intelligence and Security Informatics (ISI),*

2012 IEEE International Conference on, pages 196–201, 2012.

[2] M. J. Burge and K. W. Bowyer. *Handbook of Iris Recognition*. Springer Publishing Company, Incorporated, 2013.

[3] Z. Cao and N. A. Schmid. Fusion of operators for heterogeneous periocular recognition at varying ranges. *Pattern Recognition Letters*, 82(Part 2):170 – 180, 2016.

[4] N. Dalal and B. Triggs. Histograms of oriented gradients for human detection. In *Computer Vision and Pattern Recognition, 2005. CVPR 2005. IEEE Computer Society Conference on*, volume 1, pages 886–893, 2005.

[5] L. Flom and A. Safir. Iris recognition system, Feb. 3 1987. US Patent 4,641,349.

[6] R. Hill. Apparatus and method for identifying individuals through their retinal vasculature patterns, Aug. 22 1978. US Patent 4,109,237.

[7] J. Kannala and E. Rahtu. Bsif: Binarized statistical image features. In *Proceedings of the 21st International Conference on Pattern Recognition (ICPR2012)*, pages 1363–1366, 2012.

[8] I. Nigam, M. Vatsa, and R. Singh. Ocular biometrics: A survey of modalities and fusion approaches. *Information Fusion*, 26(Supplement C):1 – 35, 2015.

[9] A. Oliva and A. Torralba. Modeling the shape of the scene: A holistic representation of the spatial envelope. *International Journal of Computer Vision*, 42(3):145–175, 2001.

[10] U. Park, R. R. Jillela, A. Ross, and A. K. Jain. Periocular biometrics in the visible spectrum. *IEEE Transactions on Information Forensics and Security*, 6(1):96–106, March 2011.

[11] U. Park, A. Ross, and A. K. Jain. Periocular biometrics in the visible spectrum: A feasibility study. In *2009 IEEE 3rd International Conference on Biometrics: Theory, Applications, and Systems*, pages 1–6, Sept 2009.

[12] A. Sharma, S. Verma, M. Vatsa, and R. Singh. On cross spectral periocular recognition. In *2014 IEEE International Conference on Image Processing (ICIP)*, pages 5007–5011, Oct 2014.

[13] N. L. Thomas, Y. Du, and Z. Zhou. A new approach for sclera vein recognition. *Proc.SPIE,Mobile Multimedia/Image Processing, Security, and Applications*, 7708:7708 – 7708 – 10, 2010.

[14] N. T. Vetrekar, R. Raghavendra, and R. S. Gad. Low-cost multi-spectral face imaging for robust face recognition. In *2016 IEEE International Conference on Imaging Systems and Techniques (IST)*, pages 324–329, 2016.

[15] Z. Xiao, C. Guo, Y. Ming, and L. Qiang. Research on log gabor wavelet and its application in image edge detection. In *Signal Processing, 2002 6th International Conference on*, volume 1, pages 592–595 vol.1, 2002.

[16] L. Zhang, M. Yang, and X. Feng. Sparse representation or collaborative representation: Which helps face recognition? In *Computer Vision (ICCV), 2011 IEEE International Conference on*, pages 471–478, 2011.

[17] X. Zhu and D. Ramanan. Face detection, pose estimation, and landmark localization in the wild. In *2012 IEEE Conference on Computer Vision and Pattern Recognition*, pages 2879–2886, June 2012.